

Superconductivity induced by flexural modes in non σ_h -symmetric Dirac-like two-dimensional materials: A theoretical study for silicene and germanene

Massimo V. Fischetti^{1,*} and Arup Polley²

¹*Department of Materials Science and Engineering, The University of Texas at Dallas
800 W. Campbell Rd., Richardson, TX 75080*

²*Kilby Research Labs, Texas Instruments Inc., 135600 N. Central Expwy., Dallas, TX 75243*
(Dated: November 9, 2018)

In two-dimensional crystals that lack symmetry under reflections on the horizontal plane of the lattice (non- σ_h -symmetric), electrons can couple to flexural modes (ZA phonons) at first order. We show that in materials of this type that also exhibit a Dirac-like electron dispersion, the strong coupling can result in electron pairing mediated by these phonons, as long as the flexural modes are not damped or suppressed by additional interactions with a supporting substrate or gate insulator. We consider several models: The weak-coupling limit, which is applicable only in the case of gapped and parabolic materials, like stanene and HfSe₂, thanks to the weak coupling; the full gap-equation, solved using the constant-gap approximation and considering statically screened interactions; its extensions to energy-dependent gap and to dynamic screening. We argue that in the case of silicene and germanene superconductivity mediated by this process can exhibit a critical temperature of a few degrees K, or even a few tens of degrees K when accounting for the effect of a high-dielectric-constant environment. We conclude that the electron/flexural-modes coupling should be included in studies of possible superconductivity in non- σ_h -symmetric two-dimensional crystals, even if alternative forms of coupling are considered.

I. INTRODUCTION

Flexural modes (or "ZA phonons") have always been of great interest in the context of two-dimensional (2D) materials. Their role in undermining the thermodynamic stability of 2D crystals is the basis of the Mermin-Wagner theorem¹⁻⁵. Their effect on electronic transport has been investigated both in the case of 2D crystals that are symmetric under reflections on the horizontal plane of the lattice (σ_h -symmetric crystals) that permit only their weak coupling to electrons at second-order (such as graphene⁶⁻¹⁰), as well as in 'buckled' non- σ_h -symmetric crystals in which a stronger coupling is allowed at first order (such as silicene or germanene, for example^{10,11}). The reason of such interest stems from the parabolic dispersion of the ZA phonons, a peculiarity that results in divergent equilibrium occupation numbers and electron-phonon matrix elements. Recent work has shown how this parabolic dispersion is actually renormalized by their anharmonic coupling with in-plane acoustic modes, resulting in a frequency-wavevector relation $\omega^{(\text{ZA})}(q)$ proportional to q^η (where q is the magnitude of the phonon wavevector), with a 'renormalized' exponent η approximately equal to 3/2. This is sufficient to guarantee the thermodynamic stability of the crystals and to weaken significantly the second-order (two-phonon) coupling to electrons in (σ_h -symmetric crystals). On the other hand, one of us (MVF) has argued that in non- σ_h -symmetric 2D crystals that exhibit a Dirac-like electron dispersion the 'renormalized' coupling is still strong enough to affect severely the carrier mobility¹¹.

If, on the one hand, a strong electron/ZA-phonon coupling is unwelcome from an electron-transport perspective, on the other hand such a strong coupling may suggest the possibility of electron pairing and the emergence

of superconductivity. The purpose of this paper is to show that, indeed, flexural modes may lead to the formation of Cooper pairs in Dirac-like, non- σ_h -symmetric crystals. Obviously, we assume that the flexural modes are not damped or suppressed by interactions with a supporting substrate or a gate insulator, as discussed in Ref. 11. Therefore, our discussion applies to free-standing monolayers or layers interacting only weakly (such as via Van der Waals interactions) with the environment.

We organize our discussion as follows: Keeping in mind the cases of silicene and germanene as significant examples, in Sec. II we consider the consequences of the significantly different wavelength dependence of the phonon frequency and of the electron-phonon interactions considered by the 'conventional' Bardeen-Cooper-Schrieffer (BCS) theory^{12,13} and those of interest here. We emphasize the role played by Migdal's theorem¹⁴, the failure of the weak-coupling limit^{15,16} in our case, and the need to consider numerically the full gap-equation, even going beyond McMillan's empirical 'strong-coupling' formula^{17,18} towards to Eliashberg's formulation of the problem¹⁹⁻²¹. In Sec. III, we briefly review the experimental²² and theoretical status regarding the emergence of superconductivity in silicene (and also germanene^{25,26}) – both phonon-mediated^{27,28} and non-phonon-mediated^{23,24}. We then present our results using the constant-gap approximation, assuming static screening. We later extend them to the solution of the energy-dependent gap also in the case of dynamic screening and in the presence of monolayers embedded in a dielectric. Our conclusions are presented in Sec. IV and can be summarized by saying that, while not excluding alternative mechanisms that may lead to an efficient electron pairing^{29-32,34,35}, flexural modes should be considered in any study that deals

with superconductivity in Dirac-like, non- σ_h -symmetric 2D crystals.

II. THE ELECTRON/ZA-PHONON COUPLING

A. Electron-phonon interaction

The potential energy associated with the phonon-mediated electron-electron interaction we consider here has the form:

$$V^{(\text{ep})}(\mathbf{q}) = \frac{\hbar\omega(\mathbf{q})M(\mathbf{q})^2}{[E(\mathbf{k}) - E(\mathbf{k} + \mathbf{q})]^2 - \hbar^2\omega(\mathbf{q})^2}, \quad (1)$$

where \mathbf{k} is the two-dimensional electron wavevector, $E(\mathbf{k})$ is the electron dispersion, and $\omega(\mathbf{q})$ is the frequency of ZA phonons of wavevector \mathbf{q} . (We omit for simplicity the superscript ‘ZA’) In the case of non-symmetric 2D materials, the electron-phonon term originates from the first-order coupling of electrons with out-of-plane acoustic phonons and has the form:

$$M(\mathbf{q})^2 = \frac{\hbar[DK(\mathbf{k}, \mathbf{k} + \mathbf{q})]^2}{2\rho \omega(\mathbf{q}) [\epsilon(\mathbf{q}, \omega)/\epsilon_s]^2}, \quad (2)$$

where ρ is the (2D) mass density of the crystal. The interaction is assumed to be statically or dynamically screened, thanks to the factor $[\epsilon_s/\epsilon(q, \omega)]^2$, where $\epsilon(q, \omega)$ and ϵ_s are the dielectric function and static dielectric constant of the crystal, respectively. The ‘deformation potential’ $DK(\mathbf{k}, \mathbf{k} + \mathbf{q})$, is proportional to $\Delta_{\text{ZA}}q$ for ‘gapped’ non-symmetric 2D materials (Δ_{ZA} being usually called the ‘acoustic deformation potential’), whereas it is independent of energy in Dirac-like 2D materials, although with an importance dependence, $\sin(\phi/2)$, on the scattering angle ϕ , as shown in Ref. 11. At the low temperatures of interest here, the Bose-Einstein phonon-occupation term $N(\mathbf{q})$ can be ignored in Eq. (1).

B. BCS-like and non-BCS-like interaction

Despite its ‘familiar’ form, Eq. (1) hides significant differences with respect to the ‘conventional’ BCS theory. In this latter case, the matrix element $M(\mathbf{q})$ grows with increasing magnitude, q , of the wavevector of acoustic (or Debye) phonons, so that large-energy phonons control the coupling. Indeed, since their frequency grows as $c_s q$, the process is mainly controlled by zone-edge modes of the Debye frequency $\omega_D = c_s q_{\text{BZ}}$. (Here c_s is some angle-averaged acoustic velocity and $q_{\text{BZ}} = 2\pi/a_0$ the equally-angle-averaged wavevector at the edge of the Brillouin zone expressed in terms of the lattice constant a_0 .) This implies the existence of a relative large region of \mathbf{k} -space in which $|E(\mathbf{k}) - E(\mathbf{k} + \mathbf{q})| \ll \hbar\omega(\mathbf{q})$ and Eq. (1) represents an attractive interaction. Moreover, Migdal’s theorem¹⁴ guarantees that the singularities in

Eq. (1) (*i.e.*, the poles $E(\mathbf{k}) - E(\mathbf{k} + \mathbf{q}) = \pm\hbar\omega(\mathbf{q})$) give a negligible contribution, since not only $v_F \gg c_s$ in metals but, also, they occur in the small- q region in which the interaction $\sim |M(\mathbf{q})|^2$ is weak. The net result is that when considering the effective phonon-mediated electron-electron interaction, given by Eq. (1), the effect of repulsive terms and poles can be neglected and we can consider only the attractive part of the interaction:

$$V^{(\text{ep})}(\mathbf{q}) \sim - \frac{M(\mathbf{q})^2}{\hbar\omega(\mathbf{q})}. \quad (3)$$

When considering the electron/ZA-phonon interaction in gapped, parabolic, non- σ_h -symmetric 2D materials, the situation is very similar: Although the phonon frequency vanishes faster than q as $q \rightarrow 0$, the strength of the interaction grows with increasing q . Therefore, we expect a BCS-like behavior, although with a weak coupling. However, the picture is completely different when considering Dirac-like materials. In this case, the matrix element $M(\mathbf{q})$ grows with *decreasing* q , actually diverging in the limit $q \rightarrow 0$ for interactions left unscreened. Therefore, low-energy ZA-phonons control the coupling. Moreover, the singularities are not even ‘poles’ (since we are assuming $\omega(\mathbf{q}) = bq^{3/2}$) and they may give non-negligible contributions, at least in principle, so that the validity of Migdal’s theorem is not guaranteed. Of course, all this also implies that whether or not the interaction given by Eq. (1) can ever be attractive must be established with careful calculations. In any event, we expect a strong interaction at low densities, since the Fermi surface/line probes the region of a strong interaction near the phonon Γ symmetry-point (and, so, small Fermi wavevectors). This is the opposite behavior of what is seen in the conventional BCS case.

Another significant difference between our situation and those handled by the BCS theory lies in the role played by dielectric screening. In the BCS case, usually applied to metals, the large plasma frequency, much larger than the Debye frequency and the superconducting gap, justifies the use of static screening. In our systems, considering statically screened interactions would also be appropriate in the normal state: Thanks to the very low frequency of the ZA phonons of interest, the plasma frequency, even if wavevector dependent and vanishing at long wavelength (the case of 2D systems), would also be large enough to justify the full response of the electron gas. However, in the superconducting state electrons exchange an additional energy of the order of the superconducting gap at the Fermi energy, $\Delta(k_F)$. The associated frequency, $\Delta(k_F)/\hbar$, even if small in the weak-coupling regime, could overcome the plasma frequency, thus rendering dynamic effects extremely important. Therefore, we shall consider static screening at first, but we shall consider dynamically screened interactions in Sec. III D.

This discussion shows that the problem we are facing is far from being trivial. Indeed, we must face problems similar to those already discussed in the literature: The validity of Migdal’s theorem in Dirac-like materi-

als has been proven in the case of graphene by Roy and coworkers³⁶, but only for ‘conventional’ interactions whose strength grows with decreasing wavelength. In our case, it is true that the so-called ‘adiabatic’ limit is reached also at small carrier densities, since $v_F \gg c_s$. However, the role of the singularities in Eq. (1) remains unclear. (We note that Migdal’s theorem has been claimed to hold even in the anti-adiabatic regime in some cases³⁷) Interactions that grow as $1/q$ at long wavelength and that may violate Migdal’s theorem have also been considered extensively in the context of high- T_c superconductors^{38–40,42,43}. Finally, superconducting states with symmetries significantly different from the BCS s -wave pairing, as reviewed by Tsuei and Kirtley⁴⁴, may dominate the picture in our case. Indeed, as we shall see below, such mechanisms have been proposed in the case of silicene. Therefore, we shall now proceed in steps, considering increasingly complicated models to gain some insight on what role the flexural modes may play.

C. Approximations and physical models

Before proceeding, in this brief subsection we summarize physical models and approximations we have embraced throughout the paper.

First, even if/when attractive, the phonon-mediated electron-electron interaction must overcome the Coulomb repulsion whose potential energy is, in principle, given by

$$V^{(C)}(\mathbf{q}) = \frac{e^2}{2\epsilon(\mathbf{q}, \omega)q}. \quad (4)$$

This interaction presents a divergence as $q \rightarrow 0$, easily circumvented by accounting for dielectric screening, and as $q \rightarrow \infty$. This latter divergence has been shown to be removed by a many-body renormalization of the Fermi velocity³⁶ in Dirac-like materials. More generally, it is removed either by employing a high- q cutoff (here we shall use the zone-edge q_{BZ}) or the use of the the Morel-Anderson pseudopotential⁴⁵. In any event, we shall show below that the superconducting gap, $\Delta(\mathbf{k})$, vanishes at large energies, so that this issue is not critical.

Regarding the electronic band structure and phonon dispersion, we shall adopt model-dispersions assumed to be valid throughout the Brillouin zone. Therefore, for gapped, parabolic materials, we shall assume an isotropic dispersion $E(\mathbf{k}) = \hbar^2 k^2 / (2m^*)$ with an effective mass m^* , whereas for Dirac-like 2D crystals we shall assume $E(\mathbf{k}) = \hbar v_F k$. Since we are interested in a region of the Brillouin zone in which $E(\mathbf{k})$ is close to the Fermi energy, E_F , these expressions are valid as long as the Fermi energy (and so the carrier density) is low enough to be in the appropriate parabolic or linear region and, for Dirac-like materials, large enough to be left unaffected by the opening of a gap due to the spin-orbit interaction. In silicene, this interaction results in the opening of a very small gap of about 1.5 meV in the buckled

structure^{46–48} at the Dirac point. This should not affect significantly our results for electron densities larger than about $6 \times 10^8 \text{ cm}^{-2}$, in practice equivalent to an undoped/ungated case. On the contrary, for germanene, the small gap of about 2 meV predicted to occur in the planar (un-buckled) structure⁴⁹ grows to about 24 meV in the buckled structure^{46,47} and this would certainly modify the Fermi surface for densities smaller than about $1.5 \times 10^{11} \text{ cm}^{-2}$. Yet, as we shall see below, the largest values for the superconductivity gap and transition temperature will be found at densities that are within the range of validity of our model, around the high- 10^{12} /low- 10^{13} cm^{-2} . These values are large enough to be left unaffected by the spin-orbit interaction, yet small enough to be satisfactorily described by a pure Dirac-like electron dispersion.

Similarly, we shall assume a ZA-phonon dispersion of the form $bq^{3/2}$ – the parameter b being fixed by the condition $bq_{BZ}^{2/3} = \omega_D$ (≈ 5 meV for SnI and HfSe₂, 15 meV for silicene, and 9 meV for germanene) throughout the entire Brillouin zone. This latter assumption should not affect the results in any significant way, since most of the ‘action’ happens at low q . However, we should note that assuming a pure Dirac-like dispersion (and also a constant electron/ZA-phonon deformation potential) may depress the values of the calculated superconductivity gap, since the repulsive part of the phonon-mediated effective electron-electron interaction will not vanish as fast as when assuming a pure Dirac dispersion. Yet, even in this case, for densities in the range that is realistically obtained by gating or doping, our assumptions should be approximately satisfactory.

Regarding dielectric screening of both the electron-phonon and the Coulomb interaction, we have used Wunsh⁵⁰ or Stern’s⁵¹ expressions for $\epsilon(q, \omega)$ for Dirac-like and gapped (parabolic) materials, respectively. Screening of the nonpolar interaction between electrons and acoustic phonons has been discussed at length in the past, with Cardona and Christensen showing the necessity of the such a screening for the dilatation (hydrostatic) deformation potential⁵². However, Tanatar has treated all nonpolar interactions as screened 1D structures⁵³ and, more recently, such a form for dielectric screening of the electron/acoustic-phonon interaction has been considered also in 2D materials by Kaasbjerg *et al.*⁵⁴ for the *Normal* (as opposite to *Umklapp*) processes we are considering here. A ‘parochial’ but exhaustive discussion of the history behind this ‘screening problem’ is given in Ref. 55, paper that also provides several additional references. As mentioned above, we shall consider statically screened interactions at first, but we shall extend our study to include dynamic-screening effects in Sec. III D.

As mentioned before, we approximate the deformation potential $D(\mathbf{k}, \mathbf{k}')$ appearing in Eq. (1) with $\Delta_{ZA} q$ (with $q = |\mathbf{k} - \mathbf{k}'|$) for parabolic, gapped materials; for Dirac-like crystals, instead, $D(\mathbf{k}, \mathbf{k}') \approx DK_0 \sin(\phi/2)$. This is a satisfactory approximation when spin-orbit interac-

tion is ignored. However, we expect it to remain a good approximation whenever the electron energy can be approximated by a linear Dirac-like dispersion, as discussed above in the context of the band structure. The different forms taken by $D(\mathbf{k}, \mathbf{k}')$ in these two different types of materials has been discussed in Ref. 11 in the context of electron transport. We shall see below that similar considerations apply also in the context of superconductivity.

Finally, we shall limit ourselves to a simple s -wave pairing and all physical and material parameters are identical to those used in Ref.11.

D. The weak-coupling limit

As our first step, we consider the ‘usual’ BCS-like weak-coupling limit. This is a realistic approximation for the quasi-conventional case of parabolic, gapped materials; on the other hand, we shall see that it is completely inadequate in the case of Dirac-like crystals.

We start by considering the equation for the superconducting gap. In the infinite-volume normalization, this can be written as:

$$\Delta(\mathbf{k}) = - \int \frac{d\mathbf{k}'}{(2\pi)^2} V(\mathbf{k}-\mathbf{k}') \mathcal{I}(\mathbf{k}, \mathbf{k}') \frac{\Delta(\mathbf{k}')}{2W(\mathbf{k}')} \tanh\left(\frac{W(\mathbf{k}')}{2k_{\text{B}}T}\right), \quad (5)$$

where k_{B} is the Boltzmann’s constant, T the temperature, $V(q)$ is the total potential energy given by the sum of the electron-phonon and Coulomb potential energies, $V^{(\text{C})}(\mathbf{q}) + V^{(\text{ep})}(\mathbf{q})$, and $W(\mathbf{k}) = \sqrt{|E(\mathbf{k}) - E_{\text{F}}|^2 + \Delta(\mathbf{k})^2}$ is the renormalized energy measured from the Fermi level. The ‘overlap factor’ $\mathcal{I}(\mathbf{k}, \mathbf{k}')$ is assumed to be $(1 + \cos \phi)/2$, where ϕ is the scattering angle, for Dirac-like materials, unity otherwise. Thanks to the isotropy of the electronic dispersion and having assumed s -wave pairing, all quantities in the expression above depend only on the magnitude k of \mathbf{k} , and in the following the notation will be simplified accordingly.⁵⁶ In the weak-coupling limit, $\Delta(k_{\text{F}}) \ll E_{\text{F}}$, and a zero temperature, the well-known approximate solutions for the gap at the Fermi energy, $\Delta(k_{\text{F}})$, is given by:

$$\Delta(k_{\text{F}}) \approx 2\hbar\omega_{\text{D}} \exp\left(\frac{1}{\nu V_{\text{eff}}}\right), \quad (6)$$

where ν is the density of states *per spin-state* at the Fermi energy and

$$V_{\text{eff}} = \int_0^\pi \frac{d\phi}{\pi} \mathcal{I}(\phi) V[2k_{\text{F}} \sin(\phi/2)] \quad (7)$$

is the potential energy averaged over the Fermi surface/line. Of course, Eq. (6) is valid only when νV_{eff} is negative. From Eq. (5), setting the gap to zero one

obtains a similar approximate ‘weak-limit’ expression for the transition temperature:

$$k_{\text{B}}T_c \approx 1.13 \hbar\omega_{\text{D}} \exp\left(\frac{1}{\nu V_{\text{eff}}}\right). \quad (8)$$

Whenever the electron density is large enough to render static screening applicable (that is: whenever the 2D plasma frequency is larger than the phonon energy), we can express the dielectric function as:

$$\epsilon(\mathbf{q}, 0) = \epsilon_{\text{s}} \left(1 + \frac{\beta}{q}\right), \quad (9)$$

where

$$\beta = \frac{e^2 g E_{\text{F}}}{4\pi \hbar^2 v_{\text{F}}^2 \epsilon_{\text{s}}} = \frac{e^2}{2\epsilon_{\text{s}} \hbar v_{\text{F}}} \left(\frac{gn}{\pi}\right)^{1/2} \quad (10)$$

for Dirac-like materials (g is the spin and valley degeneracy), and

$$\beta = \frac{e^2 m^*}{2\pi \epsilon_{\text{s}} \hbar^2} \quad (11)$$

for gapped, parabolic materials.

For parabolic materials, let’s consider the limit $\beta \gg 2k_{\text{F}}$. Since $\beta \sim 10^{10} \text{ m}^{-1}$ for $m^* = m_0$ and $\epsilon_{\text{s}} = 10 \epsilon_0$, this condition is met at densities $n = k_{\text{F}}^2/(2\pi) \ll \beta^2/(8\pi) \sim 10^{14} \text{ cm}^{-2}$. Therefore, taking this limit should be satisfactory in all reasonable cases⁵⁷. In this limit, $\beta/(2k_{\text{F}}) \gg 1$, and recalling that the density of states (per spin state) at Fermi surface is $m^*/(2\pi\hbar^2)$, we have:

$$\nu V_{\text{eff}}^{(\text{tot})} \sim -\frac{4\Delta_{\text{ZA}}^2 k_{\text{F}} \hbar^2 \epsilon_{\text{s}}^2}{e^4 \rho b^2 m^*} + 1/2. \quad (12)$$

We have considered the two parabolic materials studied in Ref. 11: Iodine-functionalized monolayer tin, SnI, and a transition metal dichalcogenide with a stable tetragonal structure (T) at room temperature, HfSe₂. With the parameters listed in that reference, $T_c \approx 4 \text{ K}$ ($\Delta \approx 0.3 \text{ meV}$) at $n = 10^{14} \text{ cm}^{-2}$, for SnI, assuming a static dielectric constant $\epsilon_{\text{s}}=4 \epsilon_0$.

For HfSe₂, an attractive interaction is obtained only at unreasonably high (metallic) densities ($> 10^{15} \text{ cm}^{-2}$). Note that the ZA deformation potential Δ_{ZA} reported in Ref. 11 (and used here) is quite small in both materials, 1.6 eV and 1.8 eV in SnI and HfSe₂, respectively.

The transition temperature, T_c , for SnI and HfSe₂ is shown in Fig. 1 as a function of the carrier density n . Note that a high electron density is required to boost the attractive effective electron/ZA-phonon interaction, as seen in the k_{F} dependence of Eq. (12).

A final interesting observation in the context of parabolic materials can be made regarding the negligible role played by in-plane modes (LA/TA phonons). Indeed, in the same limit $\beta \gg 2k_{\text{F}}$, the electron-electron interaction energy due to the coupling with the in-plane modes takes the form:

$$\nu V_{\text{eff}}^{(\text{ep})} \sim -\frac{m^* \Delta_{\text{LA}}^2 k_{\text{F}}^2}{2\pi \hbar^2 \rho c_{\text{s}}^2 \beta^2}. \quad (13)$$

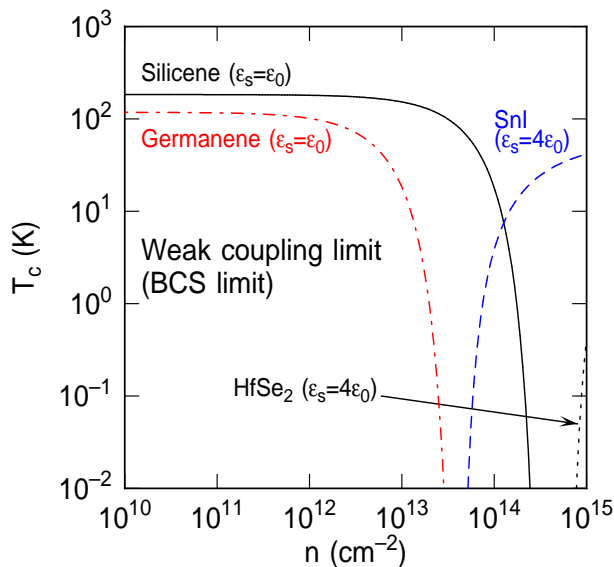


FIG. 1. Normal-superconducting transition temperature, T_c , calculated for parabolic, gapped materials (SnI and HfSe₂) and Dirac-like silicene and germanene using the weak-coupling limit. Note the usual density dependence and weak effect seen for parabolic materials in which superconductivity is expected only at unrealistically high metallic carrier densities. On the contrary, for Dirac-like materials, the large values obtained for T_c imply a failure of the weak-coupling approximation.

This quantity, rather than being of the order of unity or larger (as in the case of ZA phonons), is of the order of 10^{-2} -to- 10^{-1} at best, even at an unrealistically high ‘metallic density (10^{15} cm^{-2}) and with high deformation potentials (5 eV). At reasonable – albeit still very high – densities, $n \sim 10^{14} \text{ cm}^{-2}$, one would need $\Delta_{\text{LA}} > 25 \text{ eV}$ to reach unity for this quantity.

The main conclusion of this discussion on gapped materials is that it is indeed the strong electron/ZA-phonon coupling (due to the superlinear dispersion $\sim q^{3/2}$) that results in superconductivity, albeit at temperatures that are not too exciting and at unrealistically high – almost metallic – carrier densities. Such a relatively weak coupling and the similarity with the conventional BCS theory renders our weak-coupling estimates reliable for these gapped, non- σ_h -symmetric 2D materials.

The different form that the electron-phonon matrix element takes in Dirac-like materials results in a dramatically different picture. Here, we first consider the weak-coupling limit also for these materials. This should be viewed as no more than an exercise requiring more accurate solutions of the gap equation, since the ‘strong coupling’ results we shall find hint at a failure of this limit. Nevertheless, this exercise will show the qualitatively correct main trends.

In this case, it is customary to assume an in-plane dielectric constant equal to the dielectric constant of the surrounding environment. For free-standing layers, this assumption implies rather large value of $a = \beta/(2k_F) =$

$e^2/(2\pi\hbar v_F \epsilon_0) \approx 8.5$ for both silicene and germanene. Thus, it is reasonable to take the large- a limit also in this case. Since $\nu = k_F/(2\pi\hbar v_F)$ (density of states per spin and valley) and $\beta = ge^2 k_F/(2\pi\hbar v_F)$ (where $g=4$ is the typical valley and spin degeneracy of hexagonal Dirac-like 2D crystals), we find for the total interaction energy:

$$\nu V_{\text{eff}}^{(\text{tot})} \sim -\frac{(DK_0)^2 \hbar v_F \epsilon_0^2}{12e^4 k_F^2 \rho b^2} + \frac{1}{16}. \quad (14)$$

Using the parameters given in Ref. 11 for silicene and germanene, we find that that $\nu V_{\text{eff}}^{(\text{tot})}$ is negative for all realistic conditions. Actually, it increases with decreasing carrier density, since in the limit of zero carrier density the electron-phonon interaction becomes unscreened and diverges as $1/(k_F \beta) \sim k_F^{-2}$, whereas the the Coulomb repulsive term remain constant. With $\hbar\omega_D = 15 \text{ meV}$ for silicene and 9 meV for germanene, at a density of $10^{12} \text{ electrons/cm}^2$ we obtain $\Delta \approx 11 \text{ meV}$ and $T_c \approx 140 \text{ K}$ for silicene and $\Delta \approx 0.5 \text{ meV}$ and $T_c \approx 7 \text{ K}$ for germanene. The transition temperature, T_c , for silicene and germanene is also shown in Fig. 1 as a function of the carrier density n . As we have anticipated above, we see a behavior that is exactly the opposite of what we see in the case of parabolic materials: As we have remarked above, this is a consequence of the fact that the electron/ZA-phonon matrix element grows at longer wavelengths, actually diverging in the unscreened, zero-density limit, $q \sim 2k_F \rightarrow 0$. The fact that the transition temperature, T_c , saturates at some maximum value, $\sim \hbar\omega_D/k_B$, is just an artifact of the weak-coupling expression, Eq. (8). This comes from the initial assumption that, if the gap Δ is small, then the integral of the full gap-equation gives a contribution only over a shell of thickness $2\hbar\omega_D$ around the Fermi surface. Clearly, if the contributions come from a narrower region of \mathbf{k} -space, the weak-coupling limit misses this fact altogether. Therefore, the estimates above may be viewed as optimistic *upper bounds* for the gap and transition temperature.

E. McMillan’s strong-coupling formula

Given the strong coupling and large (unreasonable?) values of T_c we find at low densities, it is necessary to consider the expression one can obtain using Eliashberg’s theory^{19,20} in the strong-coupling limit. This theory is probably the state-of-the-art for ‘conventional’ superconductivity, although the results may differ when considering the long-wavelength coupling we have to deal with in our cases.

Deferring the task of finding a full solution of the gap equation to the next section, here we consider a ‘popular’ expression used in the strong-coupling limit. In this case, assuming a k -independent gap, the quantity of interest is the Eliashberg’s electron-phonon spectral

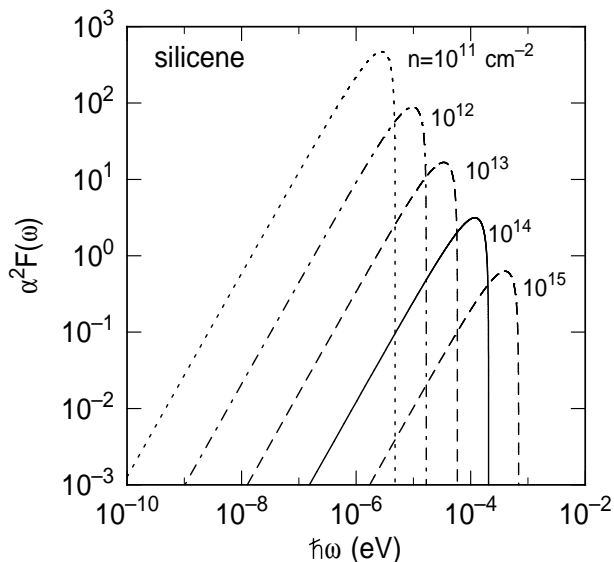


FIG. 2. Eliashberg's electron-phonon spectral function calculated as a function of frequency at various carrier densities for silicene.

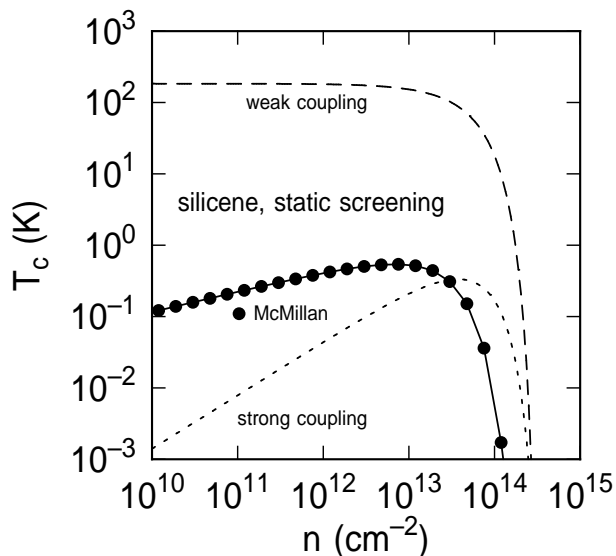


FIG. 3. Transition temperature calculated for silicene using the weak-coupling limit (dashed lines), the strong-coupling fit, Eq. (18) of the text (dotted lines), and McMillan's approximation to solve the full gap equation within the constant-gap approximation (symbols).

function^{19,20} (see also the review by Ummarino²¹):

$$\alpha^2 F(\omega) = \nu \int_0^\pi \frac{d\phi}{\pi} \frac{1 + \cos \phi}{2} \omega(q) V^{(\text{ep})}(q) \delta[\omega - \omega(q)]. \quad (15)$$

with $q = 2k_F \sin(\phi/2)$. In our case this is:

$$\alpha^2 F(\omega) = \nu \frac{2 (DK_0)^2 (\omega/\omega_F)^{4/3} [1 - (\omega/\omega_F)^{4/3}]}{3 \pi \rho \omega_F^2 [(\omega/\omega_F)^{2/3} + \beta/(2k_F)]^2}, \quad (16)$$

where $\omega_F = b(2k_F)^{3/2}$. Figure 2 shows this function at

various values of the (unrenormalized) density n . Note how this function, and so the coupling, is dominated by long-wavelength phonons, especially as n decreases.

The strength of the interaction is given by the dimensionless coupling constant:

$$\lambda = 2 \int_0^{\omega_D} d\omega \frac{\alpha^2 F(\omega)}{\omega}, \quad (17)$$

which is obviously equal to $-2\nu V_{\text{eff}}^{(\text{ep})}$.

McMillan¹⁸ has provided an empirical estimate for the transition temperature that, in a slightly revised form given by Allen and Dynes⁵⁸, takes the form:

$$k_B T_c = \frac{\hbar \omega_{\text{log}}}{1.2} \exp \left[-\frac{1.04(1 + \lambda)}{\lambda - \mu^*(1 + 0.62\lambda)} \right], \quad (18)$$

where μ^* is an effective repulsive Coulomb term. As mentioned before, this is often taken to be the Morel-Anderson potential⁴⁵. However, here we take it as $\nu V_{\text{eff}}^{(\text{C})}$. The frequency ω_{log} is the logarithmic average of the phonon frequencies involved in the coupling,

$$\omega_{\text{log}} = \exp \left[\frac{2}{\lambda} \int_0^{\omega_D} d \log(\omega) \frac{\alpha^2 F(\omega)}{\omega} \right]. \quad (19)$$

The dotted line in Fig. 3 shows this limit for silicene, compared to the weak-coupling limit. The maximum values of the transition temperature is reduced. Moreover, the qualitative features are significantly different, showing a reduction of the transition temperature at lower carrier densities, as a result of the reduced thickness of the Fermi-shell.

Ummarino²¹ has stressed the fact that the McMillan formula, Eq. (18), is no more than an empirical fit to a limited set of results that McMillan obtained solving Eliashberg's equations for a few metals^{17,18}. Therefore, we must confirm these results by tackling the harder problem of solving the full gap equation.

III. SILICENE AND GERMANENE

Here and in the following we shall consider only non- σ_h -symmetric 2D materials with a Dirac-like electron dispersion. Indeed, we have argued that the weak-coupling limit describes satisfactorily the case of parabolic, gapped materials. We consider specifically the interesting cases of silicene and germanene, since the possible emergence of superconductivity in these materials has already been studied (and even possibly experimentally observed in silicene).

A. Superconductivity in silicene

Chen *et al.*²² have reported the experimental observation of superconductivity in silicene on (111) Ag. Superconductivity has also predicted by Wan *et al.*²⁷ on the

basis of phonon-mediated processes in biaxially strained silicene. A similar study has been presented also by Durajski and co-workers²⁸, also for biaxially-strained silicene. The experimentally observed gap, Δ is about 35 meV, but it disappears at a temperatures of only 35-40 K, a gap/temperature ratio that is inconsistent with the universal prediction of the conventional BCS theory. Chen and coworkers²² speculate that this is either an artifact due to the fact the temperature of their STM tip differs significantly from the sample temperature or, instead and more intriguing, that it indicates that silicene is not an *s*-wave superconductors and conventional BCS theory does not apply. However, the experimental situation is quite complex, since measurements were performed with STM on silicene supported by (111) Ag and additional effects, such as electric-field-induced interface superconductivity⁵⁹ of Ag may also play a role. Indeed, Zhang and coworkers have speculated about electric-field-induced superconductivity for silicene²⁴ and Zhang and co-workers themselves and Liu *et al.*²³ have investigated non-*s*-wave pairing in silicene monolayers and bilayers, respectively. However, they have considered not phonon-mediated processes but, rather, an RPA multi-orbital Hubbard-model approach^{29,31-35}.

The *ab initio* calculations by Wan *et al.*²⁷ and Durajski and co-workers²⁸ are for silicene under large tensile biaxial strain and result in an estimated T_c of about 10-to-20 K at densities exceeding 10^{14} cm⁻². Unfortunately, the sophistication afforded by first-principles calculations often comes at the price of a numerical complexity that forces the use of additional approximations. For example, in Ref. 27 the very coarse mesh used to discretize the Brillouin zone (120×120) makes it impossible to capture correctly the long-wavelength behavior of the electron/ZA-phonon matrix elements, thus missing or underestimating *the* major physical effect we consider here. Moreover, the integration over the Fermi surface is performed by replacing the width of the shell with a Gaussian ‘smearing’ with a width of 0.01 Ry, an energy that is much larger than any other energy of interest in the problem. As a result, Wan *et al.* find a transition temperature that increases with increasing density, despite the fact that they identify Γ -phonons (optical and ZA) as controlling the attractive effective electron-phonon interaction. In this case (very plausible and expected, given the divergence at long wavelengths of the electron/ZA-phonon interaction), one would expect the role of these $q = 0$ -phonons to grow as the radius of the Fermi circle shrinks; that is, at low densities. We should mention that Ezawa²⁵ has also speculated about the topological-superconductor nature of some ‘popular’ non- σ_h -symmetric 2D crystals, such as silicene, germanene, and stanene. Baskaran²⁶ has similarly argued about possible room-temperature superconductivity of silicene and germanene. Given this state of affairs, it is worth revisiting the problem, following the same path that we have followed so far, attempting to capture the long-wavelength region as accurately as possible.

B. The full gap-equation

It is convenient to recast the gap equation, Eq. (5) in terms of the ‘frequency’ variables $\omega = v_F k$, $\omega' = v_F k'$, $\omega_q = b q^{3/2}$. Then, gap equation can be written as:

$$\Delta(\omega) = -\frac{1}{(4\pi v_F)^2} \int_0^{\omega_{\max}} d\omega' \omega' \frac{\Delta(\omega')}{\sqrt{\hbar^2(\omega' - \omega_F)^2 + \Delta(\omega')^2}} \\ \times \mathcal{P} \int_{\omega_{q,\min}}^{\omega_{q,\max}} d\omega_q (1 + \cos \phi) \left(\frac{d\phi}{d\omega_q} \right) V(\omega, \omega', \omega_q), \quad (20)$$

where the interaction potential is:

$$V(\omega, \omega', \omega_q) = -\frac{(DK_0)^2}{\rho} \frac{\sin^2(\phi/2)}{\omega_q^2 - (\omega' - \omega)^2} \frac{\omega_q^{4/3}}{(\omega_q^{2/3} + \omega_\beta^{2/3})^2} \\ + \frac{e^2 b^{2/3}}{\epsilon_s (\omega_q^{2/3} + \omega_\beta^{2/3})}. \quad (21)$$

In Eq. (20), \mathcal{P} denotes the Cauchy principal part of the integral, and:

$$\left\{ \begin{array}{l} \omega_{\max} = 2\pi v_F / a_0 \\ \omega_{q,\max/\min} = \frac{b}{v_F^{3/2}} |\omega' \pm \omega|^{3/2} \\ \omega_\beta = b \beta^{3/2} \\ \cos \phi = \frac{\omega^2 + \omega'^2 - (v_F^2 / b^{4/3}) \omega_q^{4/3}}{2 \omega \omega'} \\ \frac{d\phi}{d\omega_q} = \frac{4 v_F^2}{3 b^{4/3}} \frac{\omega_q^{1/3}}{2 \omega \omega' \sin \phi} \end{array} \right. \quad (22)$$

Of course, ϕ is expressed as a function of ω , ω' and ω_q , and so are $\sin^2(\phi/2) = (1 - \cos \phi)/2$ and $\sin \phi = \sqrt{1 - \cos^2(\phi)}$.

Equation (20), as well as Eq. (25) below, is a slightly simplified form of the Eliashberg’s equation (see, for example, Eq. (37b) of Ref. 19): In addition to having ignored the phonon Bose factors, consistently with the approximation embraced initially, and approximated the electron self-energy, we have also ignored corrections to the phonon self-energy. This seems to be a common approximation in the Eliashberg’s formalism, although, given the strength of the electron/ZA-phonon interaction in our case, these are corrections whose importance should be investigated. We shall ignore this issue here. Of course, in addition to these assumptions, the specific form of the electron-phonon interaction also differs, since Eliashberg considered metals with an electron-phonon matrix element growing linearly with q .

Obviously, we have not resolved the problem of the non-analyticity of the integrand function; we have simply

transferred the essential singularities from the denominator $\omega_q^2 - (\omega' - \omega)^2$ in Eq. (21) to essential singularities elsewhere, namely, the fractional powers and absolute values in Eqs. (22). However, having formulated the gap equation in terms of these new variables, we can identify the poles of the effective interaction potential, Eq. (21), and attempt a numerical approach by considering Eq. (20) simplified, as usual, by assuming an ω -independent gap and looking for the gap at the Fermi surface, $\Delta(\omega_F)$:

$$1 = -\frac{1}{(4\pi v_F)^2} \int_0^{\omega_{\max}} d\omega' \omega' \frac{1}{\sqrt{\hbar^2(\omega' - \omega_F)^2 + \Delta(\omega_F)^2}} \times \mathcal{P} \int_{\omega_{q,\min}}^{\omega_{q,\max}} d\omega_q (1 + \cos \phi) \left(\frac{d\phi}{d\omega_q} \right) V(\omega_F, \omega', \omega_q), \quad (23)$$

considering also the equation for the transition temperature, T_c :

$$1 = -\frac{1}{(4\pi v_F)^2} \int_0^{\omega_{\max}} d\omega' \omega' \frac{1}{\hbar|\omega' - \omega_F|} \tanh\left(\frac{\hbar|\omega' - \omega_F|}{2k_B T_c}\right) \times \mathcal{P} \int_{\omega_{q,\min}}^{\omega_{q,\max}} d\omega_q (1 + \cos \phi) \left(\frac{d\phi}{d\omega_q} \right) V(\omega_F, \omega', \omega_q). \quad (24)$$

Extreme care must be taken in order to treat correctly the Cauchy principal part of the integral, employing highly nonuniform meshes to discretize the ω' and ω_q integration interval.

Given the complexity of the numerical task at hand, we can confirm the correctness of our results by employing two additional strategies. The singularities can be regularized by adding an imaginary term to the phonon energy, $\omega_q \rightarrow \omega_q + i\eta$. Physically, the lifetime $1/\eta$ may be thought as caused by the anharmonic coupling to in-plane phonons. The numerical integration can then be performed in a similar way. Alternatively, we can adopt McMillan's approximation: In the denominator of Eq. (21), we retain only the term ω_q^2 when $\omega_q^2 \geq (\omega' - \omega)^2$, or retain only the term $(\omega' - \omega)^2$ when $\omega_q^2 < (\omega' - \omega)^2$.

Figure 4 shows the resulting gap (top frame) and transition temperature (bottom frame) obtained by computing the Cauchy principal part of the ω_q -integral in Eq. (23) (open circles, black), as well as the two additional approximate solutions: The solution obtained by regularizing the singularities by accounting for a finite phonon lifetime with $\eta = 10^{-6}\omega_D$ (open triangles, cyan on-line) and using McMillan's approximation (open squares, blue on-line). Note that the results obtained using these three different numerical strategies are in excellent agreement. This is a non-trivial result, since it shows – albeit indirectly – that Migdal's theorem is likely to hold even in our rather unconventional case. Figure 5 shows the superconducting gap at the Fermi energy obtained for germanene using the various approximations we have considered also for silicene.

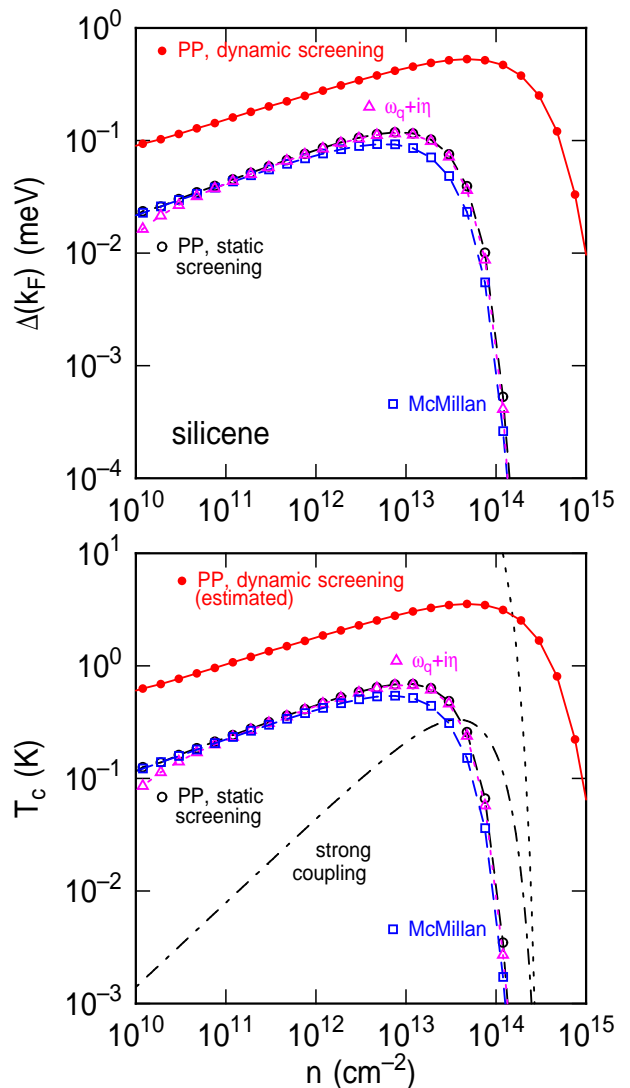


FIG. 4. Superconducting gap at the Fermi energy (top) and transition temperature (bottom) calculated for silicene using the various approximations described in the text: The weak coupling limit, the strong-coupling limit, and the solution of the gap equation (constant-gap approximation) integrating it through the singularities by computing the Cauchy principal part of the integral ('PP, static screening', black open circles); by regularizing the singularities accounting for a finite phonon lifetime, $1/\eta$, with $\eta = 10^{-6}\omega_D$ (' $\omega + i\eta$ ', open triangles, cyan on-line); and employing McMillan's approximation, as described in the text ('McMillan', open squares, blue on-line). The dots (red on-line) also show the results obtained accounting for dynamically screened interactions and calculating the Cauchy principal part of the integral.

C. The frequency-dependent gap

An assumption we have made consistently up to this point has been the 'constant gap approximation'. Given the narrow range of \mathbf{k} -space in which the effective electron-electron interaction is nonzero, we expect that this is a satisfactory approximation. More specifically,

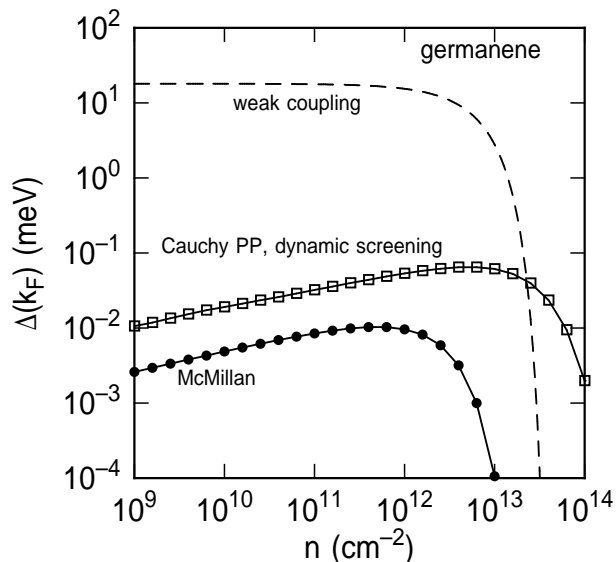


FIG. 5. Superconductivity gap for germanene calculated using some of the approximations described in the text and in Fig. 4.

we expect that the value of the gap (and transition temperature) obtained within this approximation will give some sort of average of the gap in the neighborhood of the Fermi energy. Yet, it is interesting to confirm the correctness of our expectations by solving the full integral equation, Eq. (20). Given the significant computational cost, we have ‘spot-checked’ our results in the interesting range of carrier densities that yield the highest values for the gap in silicene. The integral equation is solved iteratively, starting from an initial guess of a Gaussian $\Delta(\omega)$ with peak value given by the result of the constant-gap approximation and width given by the Debye frequency. Using the same integration mesh described above, convergence up to 10^{-6} eV is usually reached in as few as 8-to-10 iterations. As shown in the top frame of Fig. 6, at the indicated values the gap oscillates with a peak positive value at the Fermi energy that is about an order of magnitude larger than the result of the constant-gap approximation. This latter result, as expected, provides an average value. The bottom frame of Fig. 6 illustrates the renormalized quasiparticle dispersion, showing that the minimum gap away from the Fermi energy is approximately of the same magnitude obtained using the constant-gap approximation.

D. Dynamic screening

So far, we have considered interactions that are statically screened. As anticipated, we expect that dynamic screening may modify the picture in the superconducting state.

In order to account for dynamically screened interactions, we follow the standard procedure outlined, for ex-

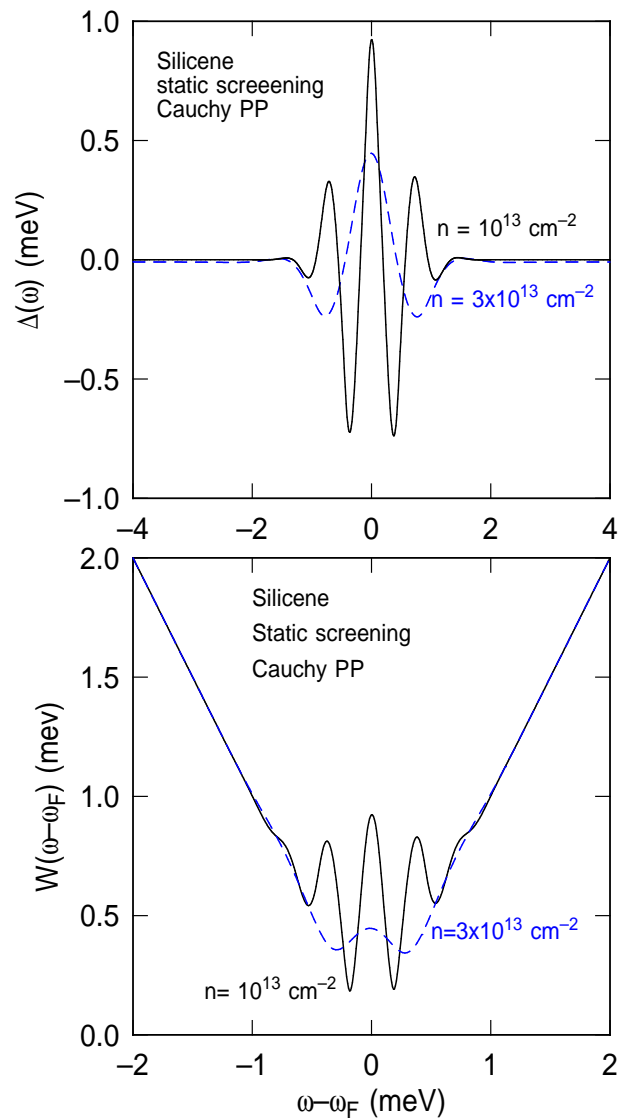


FIG. 6. Top: Superconducting gap as a function of frequency calculated by solving the integral gap equation at the indicated carrier densities. Bottom: Renormalized quasiparticle dispersion corresponding to the results shown in the top frame.

ample, in Ref. 60. We can re-express the equation for the gap $\Delta(\omega, i\omega_n)$ in terms of a sum over Matsubara frequencies ω_n and screen the interaction potential using an analytic extension of the Wunsch’ polarizability $\Pi^{(\text{RPA})}(q, \omega)$ to imaginary frequencies. Restricting our attention to the gap calculated at $\omega_n = 0$ and also assuming that it does not depend on $i\omega_n$, (an assumption that is just an extension of the ‘constant gap’ approximation we have used before), the sum over the Matsubara frequencies can be converted to an integral over the imaginary axis in the zero-temperature limit. Rotating the integration axis to real frequencies and ignoring the imaginary part of $\Delta(\omega)$,

we finally obtain:

$$\Delta(\omega) = -\frac{1}{(4\pi v_F)^2} \int_0^{\omega_{\max}} d\omega' \frac{\omega' \Delta(\omega')}{\sqrt{\hbar^2(\omega' - \omega_F)^2 + \Delta(\omega')^2}} \\ \times \mathcal{P} \int_{\omega_{q,\min}}^{\omega_{q,\max}} d\omega_q (1 + \cos \phi) \left(\frac{d\phi}{d\omega_q} \right) \\ \times \text{Re } V^{(\text{RPA})}(\omega, \omega', \omega_q; \tilde{\omega}_0). \quad (25)$$

In this equation, note the presence of the gap $\Delta(\omega')$ in the frequency $\tilde{\omega}_0 = \sqrt{(\omega' - \omega_F)^2 + \Delta(\omega')^2/\hbar^2}$ entering the RPA dielectric function. This had been anticipated in Sec. II B in our early discussion about dielectric screening.

Equation (25) evaluated at the Fermi energy, and also assuming the ‘usual’ constant-gap approximation, becomes:

$$1 = -\frac{1}{(4\pi v_F)^2} \int_0^{\omega_{\max}} d\omega' \frac{\omega'}{\sqrt{\hbar^2(\omega' - \omega_F)^2 + \Delta(\omega_F)^2}} \\ \times \mathcal{P} \int_{\omega_{q,\min}}^{\omega_{q,\max}} d\omega_q (1 + \cos \phi) \left(\frac{d\phi}{d\omega_q} \right) \\ \times \text{Re } V^{(\text{RPA})}(\omega_F, \omega', \omega_q; \tilde{\omega}_0), \quad (26)$$

where (to be explicit, just for completeness and clarity) $V^{(\text{RPA})}(\omega_F, \omega', \omega_q; \tilde{\omega}_0)$ is given by Eq. (21), but modified to account for dynamic screening:

$$V^{(\text{RPA})}(\omega_F, \omega', \omega_q; \tilde{\omega}_0) = \\ -\frac{(DK_0)^2 \sin^2(\phi/2) \omega_q^{4/3}}{\rho \omega_q^2 - (\omega' - \omega_F)^2 [\omega_q^{2/3} + \omega_\beta(\tilde{\omega}_0)^{2/3}]^2} \\ + \frac{e^2 b^{2/3}}{\epsilon_s [\omega_q^{2/3} + \omega_\beta(\tilde{\omega}_0)^{2/3}]} \\ = -\frac{(DK_0)^2 \sin^2(\phi/2) q^2}{\rho b^2 q^3 - (\omega' - \omega_F)^2 [q + \beta(\tilde{\omega}_0)]^2} \\ + \frac{e^2}{\epsilon_s [q + \beta(\tilde{\omega}_0)]}, \quad (27)$$

with $\beta(\tilde{\omega}_0) = -e^2/(2\epsilon_0 q) \Pi^{(\text{RPA})}(q, \tilde{\omega}_0)$, $\omega_\beta(\tilde{\omega}_0) = b \beta(\tilde{\omega}_0)^{3/2}$ and $q = (\omega_q/b)^{2/3}$. Unfortunately, a similar ‘simple’ equation does not hold for the transition temperature, since we have taken the zero-temperature limit to convert the sum over Matsubara frequencies to a numerically more convenient integral. Yet, the value for $\Delta(\omega_F)$ obtained by solving Eq. (26) can give us a qualitative idea of how dynamic screening may affect the normal-superconducting transition.

The results (symbols labeled ‘PP, dynamic screening’) are shown in Figs. 4 and 5 for silicene and germanene, respectively. The effect is significant: The maximum values of the superconducting gap and transition temperature are shifted at larger carrier densities, but are also increased by almost one order of magnitude, the ‘estimated’ (using the BCS ‘universal’ gap-to-temperature ratio) critical temperature reaching a value of about 5 K for silicene.

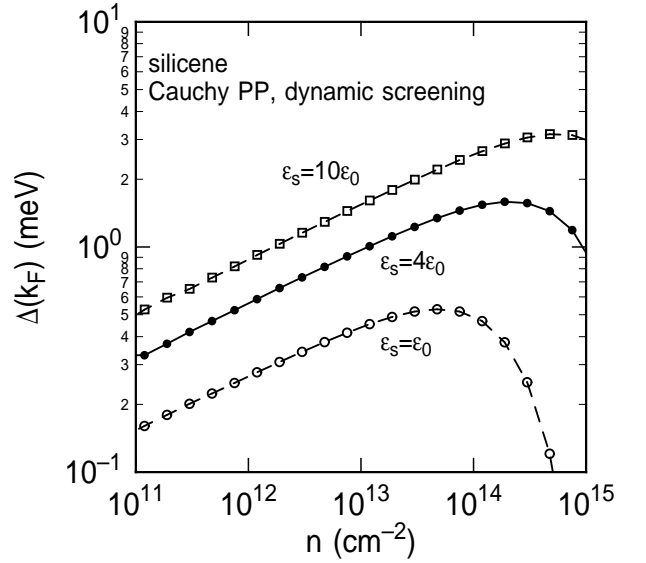


FIG. 7. Superconducting gap calculated by integrating the singularities via the Cauchy principal part and with a dynamic model for screening assuming different values for the silicene dielectric constant ϵ_s , resulting from different substrates or gate oxides.

E. Effect of the dielectric environment

All results presented so far have been obtained in the ideal case of free-standing layers. It is interesting to have a qualitative idea of what effect a substrate or gate dielectric may have on the superconducting gap. We know that the dielectric constant of 2D crystals tends to approach the value of the dielectric constant of the supporting substrate and/or of the gate insulator (or passivating layer)⁶¹. This is the result of the fact that the polarization of the 2D layer is strongly affected by the polarization of the dielectric environment itself. The dielectric response of the 2D layer will also be different along the in-plane or out-of-plane directions⁶¹. Let’s ignore these complications and, rather than tackling the hard problem of calculating the full dielectric response of the system substrate/silicene/gate insulator, let’s assume that the dielectric constant of silicene takes a value similar to the average value of the system. Therefore, we can assume that silicene supported and passivated by hBN or by SiO₂ will have an isotropic dielectric constant $\epsilon_s \approx 4 \epsilon_0$ or $\approx 10 \epsilon_0$, when supported by hBN/SiO₂ and gated by HfO₂.

Figure 7 shows the superconducting gap in these two over-simplified cases calculated using our ‘best’ model; that is: integration of the singularities by computing numerically the Cauchy principal part of the integral and employing dynamic screening. The more efficient screening of the Coulomb repulsive interaction and the reduced Thomas-Fermi screening length contribute to enhancing the gap. A maximum value of about 2-3 meV can be reached at the highest density for which our simplified

band-structure remains valid ($\sim 7 \times 10^{13} \text{ cm}^{-2}$) and also reasonably achieved in gated layers. Extrapolating from the ‘universal’ ratio $k_B T_c / \Delta(k_F) \sim 0.56$ seen in most of the cases we have considered, we can estimate that this will correspond to a transition temperature of about 15-20 K. Therefore, as long as the supporting substrate or gate insulator couple with the 2D layer via weak Van der Waals forces that do not damp or suppress the flexural modes, a ‘high-k’ environment may be beneficial as far as superconductivity is concerned.

IV. CONCLUSIONS

We have considered the strong interaction between electrons and flexural modes that is allowed at first in non- σ_h -symmetric two-dimensional crystals and its potential to induce superconducting electron pairing. We have argued that in ‘gapped’ materials that exhibit a parabolic electron dispersion, the interaction is too weak to lead to any superconductivity at realistic carrier densities. On the contrary, in 2D materials that exhibit a Dirac-like electron dispersion, the interaction is strong enough to induce superconductivity. We have shown that this interaction is significantly different from the interactions considered by the ‘conventional’ BCS theory, since its strength increases at long wavelengths. Therefore, we have investigated the strong-coupling limit using McMillan’s empirical strong-coupling (Eliashberg) formula, by solving directly the integral gap equation within

the constant-gap approximation and assuming statically-screened interactions. We have shown that the negligible role played by the singularities of the phonon-mediated electron-electron interaction suggests the validity of Migdal’s theorem in our cases. Finally, we have extended our study to account for dynamic screening, for the energy dependence of the superconducting gap, and for the presence of a dielectric environment (supporting substrate or gate insulator). We have estimated that superconductivity in silicene can exhibit a transition temperature varying from 5 K to 20 K, depending on the dielectric environment. While not ‘earth-shaking’, these results make us conclude that the electron/ZA-phonon interaction should be correctly accounted for when studying possible mechanisms leading to superconductivity in non- σ_h -symmetric, Dirac-like two-dimensional materials.

ACKNOWLEDGMENTS

The authors would like to acknowledge constructive conversations with professor Alex Demkov and Mr. Donghan Shin (The University of Texas, Austin) and with professor William Vandenberghe (The University of Texas, Dallas). This work has been partially supported by the Nanoelectronics Research Initiative’s (NRI’s) Southwest Academy of Nanoelectronics (SWAN) center affiliated with the Semiconductor Research Corporation.

* max.fischetti@utdallas.edu.

¹ R. E. Peierls, Ann. I. H. Poincaré **5**, 177 (1935).

² L. D. Landau, Phys. Z. Sowjetunion **11**, 26 (1937).

³ N. D. Mermin and H. Wagner, Phys. Rev. Lett. **17**, 1133 (1966).

⁴ P. C. Hohenberg, Phys. Rev. **158**, 383, (1967).

⁵ S. Coleman, Comm. Math. Phys. **31**, 259 (1973).

⁶ E. Mariani and F. von Oppen, Phys. Rev. Lett. **100**, 076801 (2008).

⁷ E. Mariani and F. von Oppen, Phys. Rev. B **82**, 195403 (2010).

⁸ I. V. Gornyi, V. Yu. Kachorovskii, and A. D. Mirlin, Phys. Rev. B **86**, 165413 (2012).

⁹ I. V. Gornyi, V. Yu. Kachorovskii, and A. D. Mirlin, Phys. Rev. B **92**, 155428 (2015).

¹⁰ T. Gunst, T. Markussen, K. Stokbro, and M. Brandbyge, Phys. Rev. B **93**, 035414 (2016).

¹¹ M. V. Fischetti and W. G. Vandenberghe, Phys. Rev. B **93**, 155413 (2016).

¹² J. Bardeen, L. N. Cooper, and J. R. Schrieffer, Phys. Rev. **108**, 1175 (1957).

¹³ D. Pines, Phys. Rev. **109**, 280 (1958).

¹⁴ A. B. Migdal, Sov. Phys.-JETP **7**, 996 (1958).

¹⁵ C. Kittel, “*Quantum Theory of Solids*” (Wiley, New York, 1963).

¹⁶ A. L. Fetter and J. D. Walecka, “*Quantum theory of many-particle systems*”, (Dover, New York, 2003).

¹⁷ W. L. McMillan and J. M. Rowell, Phys. Rev. Lett. **14**, 108 (1965).

¹⁸ W. L. McMillan, Phys. Rev. **167**, 331 (1968).

¹⁹ G. M. Eliashberg, Sov. Phys. JETP **11**, 696 (1960).

²⁰ G. M. Eliashberg, Sov. Phys. JETP **12**, 1000 (1961).

²¹ G. A. C. Ummarino, *Eliashberg theory*, in “*Emergent Phenomena in Correlated Matter. Modeling and Simulation*”, Vol. 3, E. Pavarini, E. Koch, and U. Schollwöck Eds. (Forschungszentrum Jülich, 2013).

²² L. Chen, B. Feng, and K. Wu, Appl. Phys. Lett. **102**, 081602 (2013).

²³ F. Liu, C.-C. Liu, K. Wu, F. Yang, and Y. Yao, Phys. Rev. Lett. **111**, 066804 (2013).

²⁴ L.-D. Zhang, F. Yang, and Y. Yao, Sci. Rep. **5**, 8203 (2015).

²⁵ M. Ezawa, J. Supercond. Nov. Magn. **29**, 1249 (2012).

²⁶ G. Baskaran, arXiv:1309.2242v3 [cond-mat.str-el] 25 Sep 2016.

²⁷ W. Wan, Y. Ge, F. Yang, and Y. Yao, Eur. Phys. Lett. **104**, 36001 (2013).

²⁸ A. P. Durajski, D. Szczśniak, and R. Szczśniak, Solid State Comm. **200**, 16 (2016).

²⁹ T. Takimoto, T. Hotta, and K. Ueda, Phys. Rev. B **69**, 104504 (2004).

³⁰ V. M. Loktev and V. M. Turkowski, Low Temperature Physics **30**, 179 (2004).

³¹ K. Yada and H. Kontani, J. Phys. Soc. Jpn. **74**, 2161 (2005).

- ³² K. Kubo, Phys. Rev. B **75**, 224509 (2007).
- ³³ I. I. Mazin, D. J. Singh, M. D. Johannes, and M. H. Du, Phys. Rev. Lett. **101**, 057003 (2008).
- ³⁴ K. Kuroki, S. Onari, R. Arita, H. Usui, Y. Tanaka, H. Kontani, and H. Aoki, Phys. Rev. Lett. **101**, 087004 (2008).
- ³⁵ S. Graser, T. A. Maier, P. J. Hirschfeld, and D. J. Scalapino, New J. Phys. **11**, 025016 (2009).
- ³⁶ B. Roy, J. Deep Sau, and S. Das Sarma, Phys. Rev. B **89**, 165119 (2014).
- ³⁷ Y. Takada, J. Phys. Soc. Jpn. **61**, 3849 (1992).
- ³⁸ M. L. Kucic and R. Zeyher, Phys. Rev. B **49**, 4395 (1994).
- ³⁹ R. Zeyher and M. L. Kucic, Phys. Rev. B **53**, 2850 (1996).
- ⁴⁰ L. Pietronero, S. Strässler, and C. Grimaldi, Phys. Rev. B **52**, 10516 (1995).
- ⁴¹ C. Grimaldi, L. Pietronero, and S. Strässler, Phys. Rev. B **52**, 10530 (1995).
- ⁴² O. V. Danylenko and O. V. Dolgov, Phys. Rev. B **63**, 094506 (2001).
- ⁴³ M. E. Palistrant and V. A. Ursu, Theor. Math. Phys. **149**, 1393 (2006).
- ⁴⁴ C. C. Tsuei and J. R. Kirtley, Rev. Mod. Phys. **72**, 969, (2000).
- ⁴⁵ P. Morel and P. W. Anderson, Phys. Rev. **125**, 1263 (1962).
- ⁴⁶ C.-C. Liu, H. Jiang, and Y. Yao, Phys. Rev. B **84**, 195430 (2011).
- ⁴⁷ C.-C. Liu, W. Feng, and Y. Yao, Phys. Rev. Lett. **107**, 076802 (2011).
- ⁴⁸ I. N. Yakovin, Surf. Sci. **662**, 1 (2017).
- ⁴⁹ R. Singh, Int. J. Mod. Phys. B, **32**, 1850055 (2018).
- ⁵⁰ B. Wunsch, T. Sauber, F. Sols, and F. Guinea, New J. Phys. **8**, 3118 (2006).
- ⁵¹ F. Stern, Phys. Rev. Lett. **18**, 546 (1967).
- ⁵² M. Cardona and N. E. Christensen, Phys. Rev. **35**, 6182 (1987).
- ⁵³ B. Tanatar, Phys. Rev. B **48**, 12001 (1993).
- ⁵⁴ K. Kaasbjerg, K. S. Thygesen, and Antti-Pekka Jauho, Phys. Rev. B **87**, 235312 (2013).
- ⁵⁵ M. V. Fischetti and S. E. Laux, Phys. Rev. B **48**, 2244 (1993).
- ⁵⁶ The gap should be evaluated as a function of the renormalized fermion density n_f in the superconducting state. In terms of the Fermi energy E_F and valley degeneracy g_v , at zero temperature this is given by:
- $$n_f = g_v \int \frac{d\mathbf{k}'}{(2\pi)^2} \left[1 - \frac{E(\mathbf{k}') - E_F}{W(\mathbf{k}')} \right].$$
- Our results show that the superconducting gap $\Delta(\mathbf{k})$ is sufficiently small to render these renormalization corrections negligible.
- ⁵⁷ Closed-form expressions valid for any value of $\beta/(2k_F)$ can easily be obtained for both parabolic and Dirac-like materials. Here we give the result only in the limit $\beta/(2k_F) \gg 1$ for simplicity, since the algebraically more complicated general results do not change the picture in any significant way.
- ⁵⁸ P. B. Allen and R. C. Dynes, Phys. Rev. B **12**, 905 (1978).
- ⁵⁹ T. Uchihashi, Superconductor Science and Technology **30**, 013002 (2017).
- ⁶⁰ I Sodemann, D. A. Pesin, and A. H. MacDonald, Phys. Rev. B **85**, 195136 (2012).
- ⁶¹ J. Fang, W. G. Vandenberghe, and M. V. Fischetti, Phys. Rev. B **94**, 045318 (2016).